Enhanced Cloud Method (E-Cloud) for Efficient Seismic Fragility Assessment of Structures

Lujie Zhuang
China University of Geosciences
Yutao Pang (pangyutaoyy@cug.edu.cn)
China University of Geosciences

Research Article

Keywords: Cloud analysis, Seismic fragility, Performance-based earthquake engineering, Structures, Nonlinear dynamic analyses

Posted Date: June 25th, 2021

DOI: https://doi.org/10.21203/rs.3.rs-647920/v1

Abstract

Cloud analysis is based on linear regression in the logarithmic space by using least squares, in which a large number of nonlinear dynamic analyses are usually suggested to ensure the accuracy of this method. So, it needs significant computational effort to establish fragility curves especially for the complicated structures. The present paper proposed the Enhanced Cloud Method (E-Cloud) to enhance the efficiency but maintain the accuracy of the Cloud method. The basic concept of the proposed “E-Cloud” aims to utilize both maximum and additional seismic responses with corresponding intensity measures (IMs) from ground motions for the logarithmic linear regression of the Cloud method. Since the nonlinear time-history responses can be transferred to the Engineering Demand Parameter (EDP)-IM curve at the duration when the ground motion is intensifying, the additional seismic responses at different IM levels (i.e., potential Cloud points) can be selected from this EDP-IM curve. These potential Cloud points are combined with maximum seismic responses for the regression so as to reduce the required number of dynamic analyses in Cloud analysis. The proposed “E-Cloud” method is applied for the case study of a typical RC frame structure. By comparison of the obtained probabilistic seismic demand models and fragility curves from “E-Cloud” method to Cloud analysis, it is demonstrated that the E-Cloud method can significantly improve the computational efficiency of the Cloud analysis, which also leads to accurate and stable results for the seismic fragility assessment of structures.

1. Introduction

Performance-based earthquake engineering (PBEE) framework has been widely used in the seismic design of structures since the Loma Prieta Earthquake (M_w= 6.9, 1989) and the Northridge Earthquake (M_w= 6.7, 1994). The identification of the structural performance helps in facilitating efficient seismic assessment and classifying the buildings designed in regions of high seismicity (Calvi et al. 2006; Jalayer et al. 2011). Fragility analysis of structures is a fundamental step in PBEE framework (Cornell and Krawinkler 2000), which is widely used for seismic performance evaluation of structures and post-earthquake management. The fragility analysis of a structure describes the probability of failure on the condition when seismic demand exceeds the structural capacity at given IM for a predefined limit state. Nowadays, there are three main approaches available in the existing literature for seismic fragility analysis to characterize the relationship between EDP and IM, namely Incremental Dynamic Analysis (IDA) (Vamvatsikos and Cornell 2002), Multiple-Stripe Analysis (MSA) (Bazzurro et al. 1998; Baker 2007; Jalayer and Cornell 2009;) and Cloud analysis (Bazzurro et al. 1998; Shome et al. 1998; Luco and Cornell 1998; Jalayer 2003). The computational effort of MSA and IDA are quite huge as repeated nonlinear dynamic analyses are needed for increasing levels of ground motion’s IM (scaled ground motions for IDA and multiple suites of scaled or unscaled ground motion with limited scale factors for MSA). Due to the simplicity of its underlying formulations (i.e., the constant dispersion and linear relationship), the Cloud method only requires fewer number of unscaled ground motions with uniformly distributed intensity levels of IM to develop the probabilistic seismic demand models (i.e., EDP-IM relationships), which is utilized to establish the fragility curves (Cornell et al. 2002; Jalayer et al. 2007; Riddell 2007; Jalayer et al. 2011; Pang et al. 2014; Billah and Alam 2015; Chen et al. 2019; Pang et al. 2020). Thus, compared to MSA and IDA, Cloud is more efficient since it only needs several nonlinear dynamic analyses based on a set of unscaled ground motions, which makes it a very popular method in seismic fragility assessment. However, since the accuracy of the linear relationship in the logarithmic scale depends on the number of regression data, a large number of unscaled ground motions are usually suggested in the previous studies for Cloud analysis. Thus, the Cloud may be computationally intensive, especially when dealing with the sophisticated finite element model of complex structures.

To reduce the computational efforts of fragility analysis, many methods have been proposed in various previous studies, such as nonlinear static procedure, machine learning techniques and Endurance Time-history Analysis (ETA). The nonlinear static procedure is proposed and developed in FEMA 273 (1997) and FEMA 356 (2000b), which has become a popular method to evaluate the seismic safety of buildings with no higher mode effect (Dutta 1999; Barron 2000; Shinozuka et al. 2000). However, it is found that the nonlinear static procedures may be unable to give the accurate assessment of fragility curves of structures (Krawinkler and Seneviratna 1998; Chi et al. 1998; Kim and D'Amore 1999; Gupta and Kunnath 2000; Goel and Chopra 2004; Chopra and Goel 2004; Maison and Hale 2004), due to the reasons that it cannot consider the damping and cyclic effects. Machine learning techniques is another powerful tool, which can replace the nonlinear time-history analysis for deriving the fragility curves after the training process. Several machine learning models (Lagaros and Fragiadakis 2007; Lagaros et al. 2009; Mitropoulou and Papadrakakis 2011; Pang et al. 2014; Mangalathu et al. 2018; Pang et al. 2021) have been demonstrated to be efficient for establishing the fragility curves. Although these models can significantly reduce the computational efforts of fragility analysis, the training process of a well-trained model can be very computationally intensive since it needs huge number of training samples generated by the nonlinear time-history analyses. In order to reduce the number of nonlinear time-history analyses required for fragility analysis, Estekanchi and Vafai (2004) proposed the ETA method, which can estimate the seismic responses of structures at various IM levels by three nonlinear time-history analyses. Unlike other traditional methods, this method adopts the endurance time acceleration functions (ETAFs) instead of a ground motion suite to consider the ground motion uncertainty. Several previous researches (Estekanchi et al. 2007; Riahi et al. 2009; Valamanesh and Estekanchi 2011; Tavazo et al. 2012; Estekanchi et al. 2020; Baniassadi and Estekanchi 2020; Amiri and Najafabadi 2020) have proven that this method is very efficient for seismic performance evaluation of structures, such as shell structures, steel moment frames and braced frames. However, the generation of ETAFs used in ETA method depends on the time-consuming unconstraint optimization algorithm, which makes this method not convenient in some cases when new ETAFs are required. In general, further study is needed to develop a new method, which can help in reducing the computational efforts and meanwhile maintain a high level of accuracy.

Similar with the ETAFs, the as-recorded ground motion also applies intensifying accelerations before the IM reaches the maximum value (IM_{max}). Moreover, based on the basic concept of the ETA method, the intensifying IM values and the corresponding structural responses before the IM_{max} can be also used to predict structural seismic behavior. Thus, in this paper, the IM vs. EDP data obtained in this intensifying period is defined as potential Cloud points, which are used as the supplementary Cloud data for the linear regression in Cloud analysis. In this way, fewer time history analyses are needed, and the computational effort for fragility assessment can be reduced considerably. This proposed method is named as "E-Cloud" for efficient seismic fragility analysis of structures. More details of "E-Cloud" method will be discussed later in this paper. The proposed method is applied in a typical reinforced concrete (RC) frame structure in this paper to demonstrate the accuracy and stability in fragility assessment.

2. Methodology

2.1 A brief overview of Cloud analysis

The Cloud analysis implements the seismic demands from a large number of nonlinear dynamic time-history analyses to establish the Probabilistic Seismic Demand Model (PSDM) as shown in **Fig. 1**. The PSDM expresses the relationship between the Engineering Demand Parameter (EDP) and IM (Cornell et al 2002) by logarithmic linear regression based on the least squares as follows.

$$E[\ln EDP \mid IM] = \ln \mu_d = \ln a + b \ln IM \quad \textbf{(1a)}$$

$$\sigma_d = \sqrt{\sum_{j=1}^{N} (\ln EDP_j - \ln \mu_d)^2 \Big/ (N-2)} \quad \textbf{(1b)}$$

where E[ln $EDP|IM$] is the expected value for the logarithm of EDP given IM;μ_d is the conditional median of EDP for a given level of IM; σ_d is the (constant) conditional logarithmic standard deviation of EDP given IM; ln a and b are parameters of linear regression;EDP_j is the EDP obtained from the j-th record and$N$ is the number of records.

Figure 1 Illustration of Cloud analysis for seismic fragility analysis

At each limit state (LS), fragility function describes the damage probability that EDP exceeds the predefined value conditional on a chosen intensity measure IM. This conditional probability is calculated as:

$$P_f[EDP \geq DS \mid IM, \eta, \beta] = \Phi\left\{\frac{\ln(\mu_d) - \ln(DS)}{\sigma_d}\right\} = \Phi\left\{\frac{\ln(IM) - \ln(\eta)}{\beta}\right\} \quad \textbf{(2)}$$

where Φ(.) is the standard normal cumulative distribution function (CDF), η and β is the median of the fragility function and the dispersion of the fragility function where ln(η) = [ln (DS)-ln(a)]/ b, $\beta = \sigma_d/b$. It is worth noting that **Eq. (2)** is a two-parameter (η and β) fragility model given IM.

2.2 The concept of the “E-Cloud” method

When establishing the PSDM, Cloud analysis usually uses the maximum seismic response from the nonlinear time-history analysis for the linear regression in the logarithmic space as shown in **Fig. 1**. This may be due to the reason that the seismic damage of structures is regarded to be directly related with the maximum seismic responses. Thus, it needs a large number of ground motions to provide sufficient data in order to ensure the quality of the regression. In this process, a large number of seismic responses are unused, which also contains valuable information on seismic behavior of structure. The main purpose of this paper is to explore how to utilize these unused structural responses for fragility assessment to reduce the computational effort.

The method to utilize the potential Cloud points is inspired by ETA. ETA method is originally proposed by Estekanchi et al. (2004), which is a dynamic pushover procedure to predict the seismic performance of structures when subjected to a few of predesigned intensifying dynamic excitations (also known as ETAFs). In the ETA method, a single ETA curve can be obtained by performing transient analysis on the finite element model for a given ETAF, as shown in Fig. 2**(a)**. It has been demonstrated by the previous studies (Estekanchi et al. 2004; Hariri-Ardebili et al. 2014) that the mean ETA curve (obtained by averaging three ETA curves) can accurately capture the seismic responses of a structural system at different seismic intensity levels, which is demonstrated by comparison to the IDA curve. Hariri-Ardebili et al. (2014) also indicated that ETA method can provide the reliable fragility estimates with fewer computational effort than IDA.

Figure 2 shows the ETAF in ETA method and the as-recorded ground motion, it can be seen from Fig. 2 that the time duration of the as-recorded ground motion (gray area in Fig. 2**(b)**) has the same characteristics as the ETAF. They both apply the intensifying dynamic excitation to the structural system. Thus, the structural responses in this duration can also reflect its seismic behavior in some extent like the ETA method. Generating the transferred EDP-IM

curve in this duration may help to predict structural responses. The method generating the transferred EDP-IM curve is the same as that in ETA method, as both two curves reflect the relationship between the maximum IM value (IM_{max}) and the maximum EDP (EDP_{max}) in [0, t], $t \subseteq [0, t_{max}]$, where t_{max} is the time when maximum IM values appears over the whole time period. Considering that both IM_{max} and EDP_{max} are time-dependent functions (denoted as $IM_{max}(t)$ and $EDP_{max}(t)$ respectively), a single transferred EDP-IM curve can be thus obtained by converting time parameter in $EDP_{max}(t)$ to IM parameter, which is shown in Fig. 2**(b)**. An averaged transferred EDP-IM curve can be obtained by averaging three transferred EDP-IM curves. For convivence, averaged transferred EDP-IM curve is abbreviated as transferred EDP-IM curve later in this paper. Note that the transferred EDP-IM curve can be used to predict structural responses of IDA curve, which is similar with the ETA method as shown in Fig. 2**(a).** Since the IDA curve is plotted with numerous IM vs. EDP points which are derived from nonlinear time history analyses, the response points (i.e., potential Cloud points) picked from the transferred EDP-IM curve can be used as the supplementary Cloud data for Cloud analysis.

Since the accuracy of Cloud analysis depends on the IM distribution of the selected ground motions (Miano et al. 2017), scattered uniformly potential Cloud points are usually required in Cloud analysis. To ensure the uniform distribution of potential Cloud points in proposed “E-Cloud” method, the ground motions used in nonlinear time history analyses should be first scaled to several predefined target IM values. Then, the transferred EDP-IM curve can be obtained further at each target IM value. It is obvious that in the transferred EDP-IM curve, the IM value of the selected potential Cloud points are smaller than the target IM value (IM_{tgt}), as shown in Fig. 3**(a)**. The potential Cloud points are picked in the region around the IM_{tgt} (shown as gray area [$a \times IM_{tgt}$, IM_{tgt}], $a \subseteq (0, 1)$ in Fig. 3**(b))**. Note that the points extraction interval should be limited specifically to avoid concentration of potential Cloud points with small IM values, thus, an appropriate value of a should be used, which will be discussed in details later. The obtained potential Cloud points based on above steps can be used to establish the PSDM, and then establish the fragility curves.

2.3 Step-by-step process for the “E-Cloud” method

Figure 4 demonstrates the flowchart of the “E-Cloud” method, which provides a step-by-step guide as follows:

1. Determine the peak IM value IM_p (e.g., peak ground acceleration (PGA) = 2.0g) of the site where the considered structure is located. Note that this IM value should be related to the maximum seismic hazard of the region.
2. Select n target IM values from 0 to IM_p to ensure uniform distribution of IM. In this paper, target IM values are chosen with constant interval as IM_p/n. For example, if IM_p=2.0g and n = 4, the target IM values are calculated as 0.5g, 1.0g, 1.5g and 2.0g. Note that the value of n has an influence on efficiency and accuracy of the “E-Cloud” method, and it will be discussed later in Sect. 4.
3. Select a suite of ground motions compatible with the seismic scenarios of the structural site. The number of the ground motion suite should be $3 \times n$. Every three ground motions should be scaled to one targe IM value with limited scale factor of 4 to avoid the excessive scaling (Davalos and Miranda 2019).
4. Establish the nonlinear finite element model of the considered structure, and conduct the nonlinear time history analyses and record the seismic responses.
5. Generate the averaged transferred EDP-IM curve for each ground motion as shown in Fig. 2**(b)**. Note that since each target IM value has three ground motions, three transferred EDP-IM curves can be generated for each target IM value. The averaged EDP-IM curve can be obtained by averaging these three transferred EDP-IM curves for each target IM value.

6. From every averaged EDP-IM curve, m potential Cloud points are picked in the range [$a \times IM_{tgt}$, IM_{tgt}] with constant IM interval, as shown in Fig. 3**(a)**. Considering that a small value of a might cause the concentration of Cloud points at low IM level, which leads to unreliable PSDM, the influence of a will be discussed in details in Sect. 4.2. The number of potential Cloud points m may also have an impact on the PSDM and fragility curves, thus it will be discussed later in Sect. 4.2 as well.
7. Develop the PSDM by $n \times m$ Cloud points, and obtain the fragility curves at different limit states.

3. Numerical Application

3.1 Building description and finite element modeling

In order to verify the proposed “E-Cloud” method, a typical six-story RC frame is selected as the case study, which is designed according to the Chinese seismic code (GB 50011 – 2010). The site condition of the considered frame is the medium-stiff soil (site-class I). This site belongs to a high seismic zone, of which the fortification intensity is 8, and the design peak ground acceleration is 0.2g. Figure 5**(a) and (b)** show the plan and elevation view of the considered RC frame respectively. Based on the regularity and symmetry of the building, the plane frame is used as the analytical object, as shown in Fig. 5**(a)**.

The 2D nonlinear finite element model of the plane frame is built in the open-source software OpenSees (McKenna et al. 2000). This finite element model employs the nonlinear force-based beam-column element with fiber sections to simulate the beams and columns. The Kent-Park model with linear tensile strength (Mohd Yassin 1994) is employed to simulate the seismic behavior of the concrete material, and the compression strength and the modulus of elasticity equal to 24.75 MPa and 2.98×104 MPa, separately. The uniaxial Menegotto-Pinto model (Filippou et al. 1983) is utilized to simulate the steel reinforcements, of which the yield strength and the modulus of elasticity are 335 MPa and 2.1×105 MPa, respectively. The confinement effect of transverse stirrups is also incorporated based on the reinforcement detailing, and the maximum compressive stress and the ultimate strain of the core concrete is increased to manifest this effect. Moreover, 5% Rayleigh damping is employed for the nonlinear time-history analysis. The fundamental mode period of the analytical model is 0.67s.

3.2 The selection of IM, EDP and limit state models

Following the recommendations from previous studies (Padgett et al. 2008; Guan et al. 2015; Hariri-Ardebili and Saouma 2016), the spectral acceleration at the fundamental period T_1 with the damping ratio of 5%, S_a (T_1, 5%), is utilized as the IM in this study. S_a (T_1, 5%) is abbreviated as S_a for convenience.

In this paper, the considered EDP is the maximum inter-story drift ratio θ_{IS}, i.e., $\theta_{IS}=u_{IS}/h$, where u_{IS} is the inter-story drift, and h is the story height. This metric has been demonstrated to be well correlated with key damage levels for the RC frame (Celik and Ellingwood 2009; Zhang and Huo 2009). Four levels of limit states (i.e., slight, moderate, extensive, and collapse) are adopted in the seismic fragility analysis. The values of θ_{IS}at various limit states are shown in **Table1**. The θ_{IS} of the RC frame at four levels of limit states was determined to be 1/550, 1/250, 1/125 and 1/50, which were obtained from the previous study (Tong and AiQun 2018).Based on the existing literatures (Nielson and DesRoches 2007; Ramanathan et al. 2012;Dezfuli and Alam 2017), the coefficients of variation (COV) are employed to describe the uncertainty for each limit state. Since high limit states usually have large uncertainties,a small value of COV (i.e., 0.25) is assigned for slight and moderatelimit states, and a large value (i.e., 0.5) is assumed for extensive and collapselimit states. The dispersion βc is calculated as $\beta_c = (\ln(1 + COV^2)$, from which the values of

0.24 and 0.47 are obtained respectively. The distribution parameters for capacity model of the RC frame are shown in **Table 1**.

Table 1
Lognormal parameters for capacity models

EDP	Slight		Moderate		Extensive		Collapse	
	$S_{c,1}$	$\beta_{c,1}$	$S_{c,2}$	$\beta_{c,2}$	$S_{c,3}$	$\beta_{c,3}$	$S_{c,4}$	$\beta_{c,4}$
θ_{IS}	1/550	0.24	1/250	0.24	1/125	0.47	1/50	0.47

3.3 Ground motion suite

In this paper, the proposed “E-Cloud” method is compared with Cloud analysis to verified its accuracy. Thus, a suite of ground motions is selected herein for Cloud analysis, which is compatible with the seismic scenario of the considered RC frame. Considering the uncertainties in the soil materials and in the ground motion characteristics, a large number of ground motions need to be adopted. Thus, a suite of 80 unscaled non-pulse-like ground motions from Baker et al. (2011) is adopted for Cloud analysis. It is a standardized suite for seismic analyses of infrastructure facilities for rock sites of California. This suite of records follows these conditions: (1) the magnitude (M_w) covers a range of between 5.7 and 7.9. (2) the closest distance-to-ruptured area (denoted as R_{RUP}) is up to around 50 km. (3) the shear-wave velocity in the top 30m (V_{s30}) varies from 620 m/s to 2000 m/s. All these conditions generally follow the RC frame site condition.

4. Results And Discussions

4.1 “E-Cloud” method procedure

As described in Sect. 2 (see the flowchart in Fig. 4), the step-by-step “E-Cloud” method procedure is given as follows:

1. Section 3.1 has mentioned the site where the considered structure is located. Based on this, the peak IM value S_a is determined as 1.0 g, which reflects the maximum seismic hazard of this region.
2. The number of target IM values n is selected as 8. The constant interval value 0.125g is obtained further, which is calculated as IM_p/n. Thus, the target IM values can be determined as 0.125g, 0.25g, 0.375g 0.5g, 0.625g, 0.75g, 0.875g and 1.0g. Note that the influence of n will be discussed later in Sect. 4.
3. Based on 8 target IM values and the limited scale factor of 4, 24 ground motions are selected randomly from a large number of records, which is compatible with the seismic scenarios mentioned in Sect. 3.1. Table 3 shows these 24 selected ground motions in 8 groups (three in each group) with the corresponding target IM values.
4. The nonlinear finite element model of the considered structure is established (Sect. 3.1). Nonlinear time history analyses are performed under selected 24 selected ground motions (Step 3) in this step to obtain the structural responses.
5. As described in the Sect. 2, the transferred EDP-IM curve can be obtained following these steps: (a) find the time t_{max}, (b) calculate the $IM_{max}(t)$ and $EDP_{max}(t)$ respectively in $[0, t_{max}]$ and (c) plot the transferred EDP-IM curve ($IM_{max}(t)$ vs. $EDP_{max}(t)$). Based on these steps, 24 transferred EDP-IM curves can be obtained. 8 averaged transferred EDP-IM curves can be then obtained by averaging every three transferred EDP-IM curves at the same target IM value.

6. Select 10 potential Cloud points from every single averaged transferred EDP-IM curve in the range [0.3×IM_{tgt}, IM_{tgt}] with constant IM interval. In this step, the parameter *a* and *m* are selected as 0.3 and 10 separately, of which the influence will be discussed later in this study.
7. In this step, PSDM is developed by the obtained 80 potential Cloud points, and fragility curves are then derived based on the limit states defined in Table 1.

Cloud analysis is applied herein as comparison to verify the accuracy of "E-Cloud" method for establishing PSDM and fragility curves. In Cloud analysis, 80 nonlinear time history analyses are conducted with the ground motion suite mentioned in Sect. 3.3, and a large number of Cloud data is thus obtained. Figure 6**(a)** shows the scatter plots (in the natural logarithmic scale) for Cloud data and the result of linear regression. The estimated parameters (*a*, *b*, and $\beta_{EDP|IM}$) of PSDMs, as well as the coefficients of determination R^2 for the considered EDP are listed in Table 2. Based on the **Eq. (1), (2)**, the fragility curves for four levels of limit states can be obtained further, as shown in Fig. 6**(b)**.

Table 2
The regression parameters of PSDM

EDP	a $\beta_{c,1}$	b $\beta_{c,2}$	$\beta_{EDP\|IM}$	R^2
θ_{IS}	1.0887	-4.6400	0.1896 0.47	0.9380

The PSDM and fragility curves at four damage levels for "E-Cloud" method are shown in Fig. 7. Figure 7**(a)** shows dispersion ($\beta_{D|IM}$) for linear regression, coefficient of determination (R^2), slope (*b*) and intercept(*a*) in PSDM for Cloud method and "E-Cloud" method separately. The value of $\beta_{D|IM}$ in E-Cloud method is smaller than that in Cloud method, as the regression data are chosen from fewer ground motions in E-Cloud method. Due to the same reason, the coefficient of determination (R^2), which is used to quantify the correlations between the studied EDPs in the logarithm space, is smaller in "E-Cloud" method than that in Cloud method. As shown in Fig. 7**(a)**, slope (*b*) and intercept (*a*) in "E-Cloud" method, which are used in establishing fragility curves, are close to the results of Cloud analysis. Figure 7**(b)** shows the fragility curves generated by both "E-Cloud" and Cloud method. It indicates that the fragility curves established in "E-Cloud" method fit well with the results of Cloud analysis. The values of median fragility for Cloud analysis and "E-Cloud" method are shown in Fig. 7**(c)**, which demonstrates the high level of accuracy of "E-Cloud" method in fragility assessment.

Table 3
Detailed information of the selected ground motion

Target IM	NGA Record Number	Earthquake Name	Year	Station	Magnitude	Hypocentral Distance	Closest Distance	Preferred Vs30 (m/s)
0.125g	1626	Sitka, Alaska	1972	Sitka Observatory	7.68	45.40	34.61	659.6
	572	Taiwan SMART1(45)	1986	SMART1 E02	7.30	72.91	-	659.6
	769	Loma Prieta	1989	Gilroy Array #6	6.93	39.54	18.33	663.3
0.25g	1485	Chi-Chi, Taiwan	1999	TCU045	7.62	77.91	26	704.6
	769	Loma Prieta	1989	Gilroy Array #6	6.93	39.54	18.33	663.3
	150	Coyote Lake	1979	Gilroy Array #6	5.74	9.12	3.11	663.3
0.375g	1013	Northridge-01	1994	LA Dam	6.69	21.10	5.92	629
	765	Loma Prieta	1989	Gilroy Array #1	6.93	33.55	9.64	1428
	72	San Fernando	1971	Lake Hughes #4	6.61	27.46	25.07	821.7
0.5g	1619	Duzce, Turkey	1999	Mudurnu	7.14	43.83	34.30	659.6
	1549	Chi-Chi, Taiwan	1999	TCU129	7.62	16.27	1.84	664.4
	1618	Duzce, Turkey	1999	Lamont 531	7.14	31.07	8.03	659.6
0.625g	810	Loma Prieta	1989	UCSC Lick Observatory	6.93	23.93	18.41	714
	1787	Hector Mine	1999	Hector	7.13	30.38	11.66	684.9
	1091	Northridge-01	1994	Vasquez Rocks Park	6.69	41.90	23.64	996.4
0.75g	1013	Northridge-01	1994	LA Dam	6.69	21.10	5.92	629
	80	San Fernando	1971	Pasadena - Old Seismo Lab	6.61	41.27	21.50	969.1
	1596	Chi-Chi, Taiwan	1999	WNT	7.62	16.27	1.84	664.4
0.875g	765	Loma Prieta	1989	Gilroy Array #1	6.93	33.55	9.64	1428
	809	Loma Prieta	1989	UCSC	6.93	24.05	18.51	714

Target IM	NGA Record Number	Earthquake Name	Year	Station	Magnitude	Hypocentral Distance	Closest Distance	Preferred Vs30 (m/s)
	1165	Kocaeli, Turkey	1999	Izmit	7.51	16.86	7.21	811
1.0g	763	Loma Prieta	1989	Gilroy - Gavilan Coll.	6.93	33.84	9.96	729.7
	150	Coyote Lake	1979	Gilroy Array #6	5.74	9.12	3.11	663.3
	1549	Chi-Chi, Taiwan	1999	TCU129	7.62	16.27	1.84	664.4

4.2 Sensitivity analysis

As mentioned in Sect. 2, the values of *a, m and n* may have an influence on the results of the “E-Cloud” method. Thus, sensitivity analysis is carried out in this section to investigate the effect of parameters *n*, *m* and *a* on PSDMs and fragility estimates.

Three levels of parameter *a*, namely 0, 0.3 and 0.5 are used in “E-Cloud” method to study the sensitivity to this parameter. Note that the variation of the parameter *a* means that the potential Cloud points are selected in the range [0, IM_{tgt}], [0.3×IM_{tgt}, IM_{tgt}] and [0.5×IM_{tgt}, IM_{tgt}] respectively. Figure 8 and Fig. 9 show the PSDM and fragility curves when *a* is selected as 0 and 0.5 respectively. And the results when $a = 0.3$ is shown in Fig. 7. By comparison of the median fragilities, it is found that all three levels of *a* yield reliable fragility assessment. However, when *a* is very small (e.g., $a = 0$ in Fig. 8), concentration of potential Cloud points may occur, and extremely small potential Cloud points can be included from the transferred EDP-IM curves at small IM target values, leading to incorrect fragility estimates at low limit states. For example, due to the concentration of potential Cloud points as shown Fig. 8**(a)**, the error − 1.57% in Fig. 9**(c)** at LS_1 increase to -9.97% in Fig. 8**(c)**, and the error − 2.45% at LS_2 increase to -5.69%. Thus, the parameter *a* should be set to an appropriate value (0.3 recommended in this paper) to avoid the concentration of potential Cloud points and extremely small potential Cloud points at small IM levels.

Three levels of *m* (i.e., $m = 5$, 10 and 20) are selected in the procedure of “E-Cloud” method to study the sensitivity to parameter *m*, which is the number of the selected potential Cloud points from a single transferred EDP-IM curve. Figure 10 and Fig. 11 illustrate PSDM and fragility curves when *m* is 5 and 20, and the results when m is 10 is shown in Fig. 7. By comparison of Fig. 11**(c)** and Fig. 7**(c)**, it is found that the error at LS_2, LS_3 and LS_4 when $m = 20$ increase from − 3.81%, -2.07% and 0.28% to -4.63%, -3.60% and − 2.22% when $m = 10$. The error at LS_1 decrease from − 5.76% to -5.79%. By comparison of Fig. 7**(c)** and Fig. 10**(c)**, the error at LS_2, LS_3 and LS_4 when $m = 10$ increase from − 4.63%, -3.60% and − 2.22% to -5.79%, -6.56% and − 7.55% when $m = 5$. The error at LS_1 decrease from − 5.79% to -4.93%. It is concluded that more potential Cloud points lead to more accurate fragility curves. Note that the value of *m* has no effect on the computational effort as the number of nonlinear time-history analyses does not change. Thus, *m* can be set as a relatively large value to ensure the accuracy of “E-Cloud” method.

Three levels of n, namely $n = 2$, $n = 4$ and $n = 8$, are used in the procedure of “E-Cloud” method respectively to investigate the influence of parameter *n*. When $n = 2$, 6 ground motions are selected and scaled to target IM values of 0.5g and 1.0g. When $n = 4$, 12 ground motions are selected and scaled to target IM values of 0.25g, 0.5g 0.75g and 1.0g. And when $n = 8$, 24 ground motions are selected and scaled to target IM values of 0.125g, 0.25g, 0.375g 0.5g,

0.625g, 0.75g, 0.875g and 1.0g. It is worth noting that in order to avoid the inaccurate linear regression due to insufficiency of Cloud data, the total number of selected potential Cloud points for case $n = 2$, case $n = 4$ and $n = 8$ should be consistent, thus, m is set as 40, 20 and 10 respectively for case $n = 2$, case $n = 4$ and case $n = 8$. Figure 12 and Fig. 13 show the PSDM and fragility curves separately for case $n = 2$ and case $n = 4$. And the results of case $n = 8$ is shown in Fig. 7. By comparison of case $n = 2$ (see Fig. 12**(c)**), case $n = 4$ (see Fig. 13**(c)**) and case $n = 8$ (see Fig. 7**(c)**), the error at LS_1 is -1.37%, -1.92% and − 5.79% separately, the error at LS_2 is -1.66%, -3.18% and − 4.63% separately, the error at LS_3 is -1.92%, -4.27% and − 3.60% separately, the error at LS_4 is -2.25%, -5.69% and − 2.22% separately. It is found that all three cases have a high level of accuracy, and this phenomenon is inconsistent with what Cloud analysis suggest (i.e., a larger number of ground motions are usually required for linear regression to establish accurate fragility curves). Considering the inherent randomness of ground motions and structural responses, it is necessary to discuss the stability of "E-Cloud" for fragility assessment in these three cases (see Sect. 4.3).

4.3 Stability of "E-Cloud" method

Since a small number of ground motions are adopted in the E-Cloud method, different ground motions may have significant effect on the E-Cloud method. Thus, in this section, the stability of this method is also investigated. In the stability analysis, ground motions are randomly selected from the ground motion suite (see Sect. 3.3) for five times and perform "E-Cloud" method to obtain fragility curves at four limit states for case $n = 2$, case $n = 4$ and case $n = 8$. The fragility curves (blue lines) for three cases are shown in Fig. 14. The results of Cloud analysis (red line) with ± 10% interval (gray region) is also shown in Fig. 14 as comparison.

It is found that when n is 2 (i.e., 6 ground motions are selected), the fragility curves perform stable and accurate (within 5% error) only at LS_1, and unstable and inaccurate results occur at LS_2, LS_3 and LS_4. When n is 4 (i.e., 12 ground motions are selected), the accuracy and stability of the fragility curves at four limit states perform better than case $n = 2$, and the errors at LS_1, LS_2 and LS_3 are around 10%, the errors at LS_4 are around 20%. In case $n = 8$, where 24 ground motions are selected, the errors of fragility curves at LS_1, LS_2 and LS_3 are around 5%, which is considered as a high level of accuracy, and at LS_4, the errors are around 15%, which is much smaller than case $n = 2$ and case $n = 4$. Conclusion can be drawn that in "E-Cloud" method, a larger value of n (i.e., more ground motions are selected) leads to more accurate and stable fragility curves, and the results at LS_1, LS_2 and LS_3 perform much better than that at LS_4, the reason for this phenomenon is due to the considerable uncertainty of structural responses at collapse limit state. Thus, at LS_1, LS_2 and LS_3, a relatively small value of n (4 in this study) is enough for accurate and stable fragility assessment (i.e., with errors around 10%), and a large value of n (8 in this study) is suggested when establishing fragility curves at collapse limit state.

Note that, in the case $n = 2$ in Sect. 4.2, the fragility curves perform accurate and stable at all four limit states (see Fig. 12), the reason may be that the selected 6 ground motions (as shown in Table 3 with target IM values 0.5g and 1.0g) have specific properties for accurate fragility assessment. Therefore, further research is needed to investigate the properties of these ground motions, which can help to reduce the computational effort considerably.

5. Conclusion

The present paper proposes the enhanced Cloud method (E-Cloud) to significantly reduce the computational effort of the Cloud method. In the E-Cloud method, the structural responses in the duration when ground motions apply intensifying dynamic acceleration are utilized (with its corresponding IM) as the supplementary Cloud data for fragility assessment. The key step of the E-Cloud method is to establish the transferred EDP-IM curves in this specific

time duration with predefined target IM values. From these transferred EDP-IM curves, the potential Cloud points can be selected and used in Cloud analysis. In general, the proposed E-Cloud method is efficient as it requires fewer nonlinear time history analyses than Cloud method.

By using a typical RC frame as a case study, the sensibility of the proposed E-Cloud is studied. The results from the sensitivity analysis indicates that appropriate points extraction interval in transferred EDP-IM curve helps in improving accuracy, as it leads to uniformly distribution of potential Cloud points, and the number of potential Cloud points selected from this interval is recommended to be large enough since it improves the accuracy with no additional computational effort. Furthermore, a larger number of ground motions leads to more accurate and stable fragility curves. The stability analysis of “E-Cloud” method demonstrates that 12 ground motions lead to stable and accurate results at slight, moderate and extensive limit states, and when establishing fragility curve at collapse limit state, 24 ground motions are recommended. Thus, following the suggestions in parameters determination and ground motions selection, the proposed “E-Cloud” method can provide stable and accurate fragility assessment with high efficiency.

In some cases, few ground motions (e.g., 6 ground motions in Sect. 4.2) can produce reliability fragility estimates. This may be due to the reason that these ground motions may have some unknown properties. Therefore, further research may be needed to explore what ground motions properties can lead to reliable fragility estimates and how to select these ground motions.

Declarations

Acknowledgements:

This research was supported by National Natural Science Foundation of China (No. 51708527)

References

1. Amiri HA, Najafabadi EP, Estekanchi HE, Ozbakkaloglu T (2020) Performance-based seismic design and assessment of low-rise steel special moment resisting frames with block slit dampers using endurance time method. Eng Struct 224:110955
2. Baker JW (2007) Probabilistic structural response assessment using vector-valued intensity measures. Earthquake Engineering Structural Dynamics 36:1861–1883
3. Baker JW, Lin T, Shahi SK, Jayaram N (2011) New ground motion selection procedures and selected motions for the PEER transportation research program. PEER report 3. Pacific Earthquake Engineering Research Center, University of California, Berkeley
4. Baniassadi A, Estekanchi H (2020) Application of endurance time method in damage assessment of concrete moment frames. International Journal of Numerical Methods in Civil Engineering 5:1–11
5. Barron R, Reinhorn A, Ayala A (2000) Spectral evaluation of seismic fragility of structures. Ph. D. Dissertation, State University of New York, Buffalo, USA
6. Bazzurro P, Cornell CA, Shome N, Carballo JE (1998) Three proposals for characterizing MDOF nonlinear seismic response. J Struct Eng 124:1281–1289
7. Billah AHM, Alam MS (2015) Seismic fragility assessment of concrete bridge pier reinforced with super-elastic shape memory alloy. Earthquake Spectra 31:1515–1541

8. Calvi GM, Pinho R, Magenes G, Bommer JJ, Restrepo-Vélez LF, Crowley H (2006) Development of seismic vulnerability assessment methodologies over the past 30 years. ISET journal of Earthquake Technology 43:75–104
9. Celik OC, Ellingwood BR (2009) Seismic risk assessment of gravity load designed reinforced concrete frames subjected to Mid-America ground motions. Journal of structural engineering 135:414–424
10. Chen X, Li J, Guan Z (2020) Fragility analysis of tall pier bridges subjected to near-fault pulse-like ground motions. Struct Infrastruct Eng 16:1082–1095
11. Chi WM, El-Tawil S, Deierlein GG, Abel JF (1998) Inelastic analyses of a 17-story steel framed building damaged during Northridge. Eng Struct 20:481–495
12. Chopra AK, Chintanapakdee C (2004) Evaluation of modal and FEMA pushover analyses: vertically “regular” and irregular generic frames. Earthquake Spectra 20:255–271
13. Cornell CA, Jalayer F, Hamburger RO, Foutch DA (2002) Probabilistic basis for 2000 SAC federal emergency management agency steel moment frame guidelines. Journal of structural engineering 128:526–533
14. Cornell CA, Krawinkler H (2000) Progress and challenges in seismic performance assessment. PEER Center News 3:1–3
15. Dávalos H, Miranda E (2019) Evaluation of the scaling factor bias influence on the probability of collapse using $S_a(T_1)$ as the intensity measure. Earthquake Spectra 35:679–702
16. Dezfuli FH, Alam MS (2017) Effect of different steel-reinforced elastomeric isolators on the seismic fragility of a highway bridge. Struct Control Health Monit 24:e1866
17. Dutta A (1999) On energy based seismic analysis and design of high way bridges. Ph.D. Dissertation, State University of New York, Buffalo, USA
18. Estekanchi HE, Mashayekhi M, Vafai H, Ahmadi G, Mirfarhadi SA, Harati M (2020) A state-of-knowledge review on the endurance time method. Structures 27:2288–2299
19. Estekanchi HE, Vafai A, Sadeghazar M (2004) Endurance time method for seismic analysis and design of structures. Sci Iran 11:361–370
20. Estekanchi HE, Valamanesh V, Vafai A (2007) Application of endurance time method in linear seismic analysis. Eng Struct 29:2551–2562
21. FEMA (1997) “NEHRP guidelines for the seismic rehabilitation of buildings.” Publ. No. 273, prepared by the Applied Technology Council for the Building Seismic Safety Council, Washington, D.C
22. FEMA (2000b) “Prestandard and commentary for the seismic rehabilitation of buildings.” Publ. No. 356, prepared by the American Society of Civil Engineers for the Federal Emergency Management Agency, Washington, D.C
23. Filippou FC, Bertero VV, Popov EP (1983) Effects of bond deterioration on hysteretic behavior of reinforced concrete joints. Report EERC 83 – 19, Earthquake Engineering Research Center, University of California, Berkelery
24. Goel RK, Chopra AK (2004) Evaluation of modal and FEMA pushover analyses: SAC buildings. Earthquake spectra 20:225–254
25. Guan M, Du H, Cui J, Zeng Q, Jiang H (2015) Optimal ground motion intensity measure for long-period structures. Meas Sci Technol 26:105001
26. Gupta B, Kunnath SK (2000) Adaptive spectra-based pushover procedure for seismic evaluation of structures. Earthquake spectra 16:367–391

27. Hariri-Ardebili MA, Saouma VE (2016) Probabilistic seismic demand model and optimal intensity measure for concrete dams. Struct Saf 59:67–85
28. Hariri-Ardebili MA, Sattar S, Estekanchi HE (2014) Performance-based seismic assessment of steel frames using endurance time analysis. Eng Struct 69:216–234
29. Ibarra LF, Medina RA, Krawinkler H (2005) Hysteretic models that incorporate strength and stiffness deterioration. Earthquake engineering structural dynamics 34:1489–1511
30. Jalayer F (2003) Direct probabilistic seismic analysis: implementing non-linear dynamic assessments (Doctoral dissertation, Stanford University)
31. Jalayer F, Cornell CA (2009) Alternative non-linear demand estimation methods for probability-based seismic assessments. Earthquake Engineering Structural Dynamics 38:951–972
32. Jalayer F, Elefante L, Iervolino I, Manfredi G (2011) Knowledge-based performance assessment of existing RC buildings. J Earthquake Eng 15:362–389
33. Jalayer F, Franchin P, Pinto PE (2007) A scalar decision variable for seismic reliability analysis of RC frames. Special issue of Earthquake Engineering Structural Dynamics on Structural Reliability 36:2050–2079
34. Kim S, D'Amore E (1999) Push-over analysis procedure in earthquake engineering. Earthquake Spectra 15:417–434
35. Krawinkler H, Seneviratna GDPK (1998) Pros and cons of a pushover analysis of seismic performance evaluation. Engineering structures 20:452–464
36. Lagaros ND, Fragiadakis M (2007) Fragility assessment of steel frames using neural networks. Earthquake Spectra 23:735–752
37. Lagaros ND, Tsompanakis Y, Psarropoulos PN, Georgopoulos EC (2009) Computationally efficient seismic fragility analysis of geostructures. Comput Struct 87:1195–1203
38. Luco N, Cornell CA (1998) Seismic drift demands for two SMRF structures with brittle connections. Structural Engineering World Wide paper T158–3
39. Maison BF, Hale TH (2004) Case study of a Northridge welded steel momentframe building having severed columns. Earthquake Spectra 203:951–973
40. Mangalathu S, Heo G, Jeon JS (2018) Artificial neural network based multi-dimensional fragility development of skewed concrete bridge classes. Eng Struct 162:166–176
41. McKenna F, Fenves GL, Scott MH (2000) Open system for earthquake engineering simulation (OpenSees). University of California, Berkeley
42. Miano A, Jalayer F, Ebrahimian H, Prota A (2018) Cloud to IDA: Efficient fragility assessment with limited scaling. Earthquake Engineering Structural Dynamics 47:1124–1147
43. Mitropoulou CC, Papadrakakis M (2011) Developing fragility curves based on neural network IDA predictions. Eng Struct 33:3409–3421
44. Mohd Yassin MH (1994) Nonlinear analysis of prestressed concrete structures under monotonic and cyclic loads. Ph.D. Dissertation, University of California, Berkeley, USA
45. Nielson BG, DesRoches R (2007) Seismic fragility methodology for highway bridges using a component level approach. Earthq Eng Struct Dyn 36:823–839
46. Padgett JE, Nielson BG, DesRoches R (2008) Selection of optimal intensity measures in probabilistic seismic demand models of highway bridge portfolios. Earthquake engineering structural dynamics 37:711–725

47. Pang Y, Dang X, Yuan W (2014) An artificial neural network based method for seismic fragility analysis of highway bridges. Advances in Structural Engineering 17:413–428
48. Pang Y, Wei K, Yuan W (2020) Life-cycle seismic resilience assessment of highway bridges with fiber-reinforced concrete piers in the corrosive environment. Eng Struct 222:111120
49. Pang Y, Wu X, Shen G, Yuan W (2014) Seismic fragility analysis of cable-stayed bridges considering different sources of uncertainties. J Bridge Engineering 19:04013015
50. Pang Y, Zhou X, He W, Zhong J, Hui O (2021) Uniform design–based Gaussian process regression for data-driven rapid fragility assessment of bridges. J Struct Eng 147:04021008
51. Ramanathan K, DesRoches R, Padgett JE (2012) A comparison of pre- and post-seismic design considerations in moderate seismic zones through the fragility assessment of multispan bridge classes. Eng Struct 45:559–573
52. Riahi HT, Estekanchi HE, Vafai A (2009) Endurance time method-application in nonlinear seismic analysis of single degree of freedom systems. J Appl Sci 9:1817–1832
53. Riddell R (2007) On ground motion intensity indices. Earthquake Spectra 23:147–173
54. Shinozuka M, Feng MQ, Kim H, Uzawa T, Ueda T (2000) Statistical analysis of fragility curves. Tech. Rep., Multidisciplinary Center for Earthquake Engineering Research, The State University of New York, Buffalo, USA
55. Shome N, Cornell CA, Bazzurro P, Carballo JE (1998) Earthquakes, records, and nonlinear responses. Earthq Spectra 14:469–500
56. Tavazo H, Estekanchi HE, Kaldi P (2012) Endurance time method in the linear seismic analysis of shell structures. International Journal of Civil Engineering 10:169–178
57. Valamanesh V, Estekanchi HE (2011) Endurance time method for multi-component analysis of steel elastic moment frames. Scientia Iranica 18:139–149
58. Vamvatsikos D, Cornell CA (2002) Incremental dynamic analysis. Earthq Eng Struct Dyn 31:491–514
59. Zhang J, Huo Y (2009) Evaluating effectiveness and optimum design of isolation devices for highway bridges using the fragility function method. Eng Struct 31:1648–1660
60. Zhou T, Li AQ, Wu YF (2018) Copula-based seismic fragility assessment of base-isolated structures under near-fault forward-directivity ground motions. Bull Earthq Eng 16:5671–5696

Figures

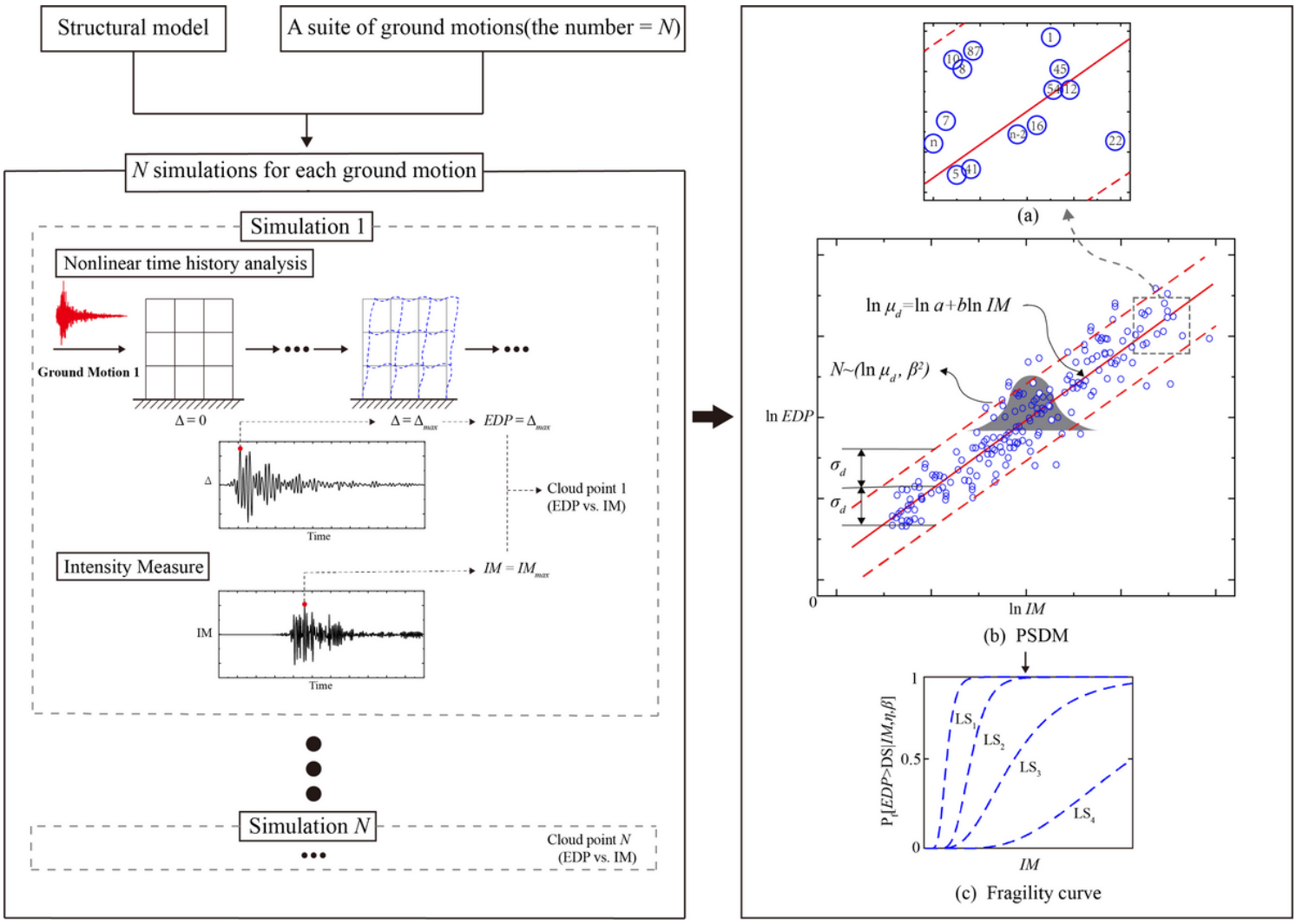

Figure 1

Illustration of Cloud analysis for seismic fragility analysis

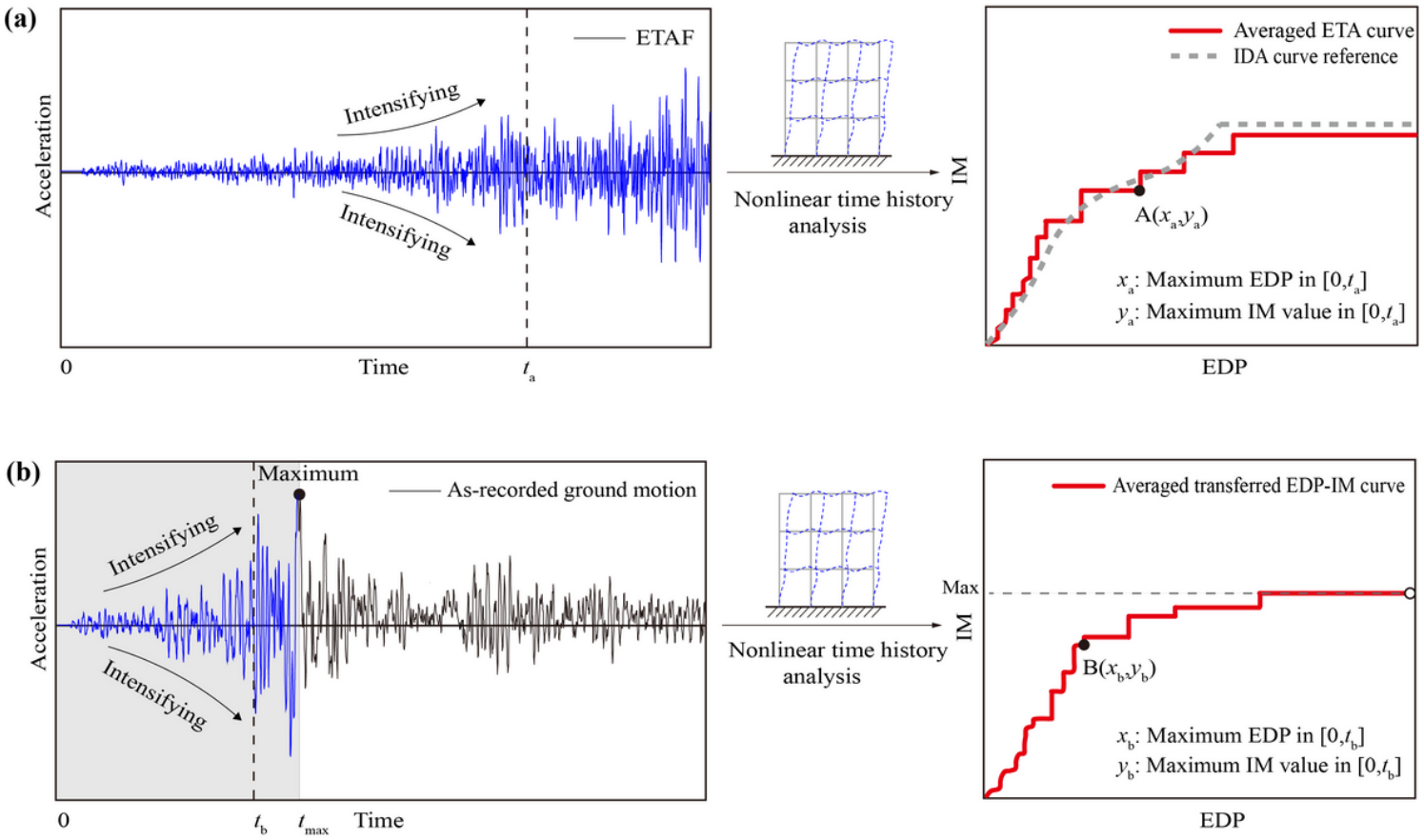

Figure 2

Similarity between ETA method and “E-Cloud” method

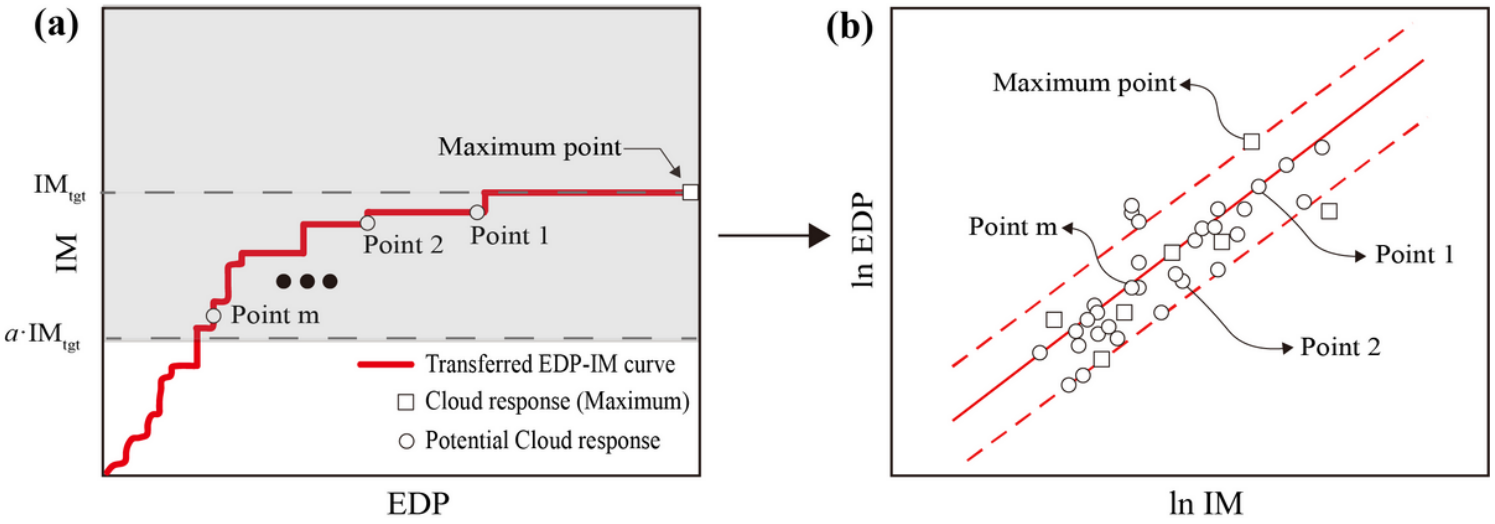

Figure 3

Establishment of PSDM by “E-Cloud” method

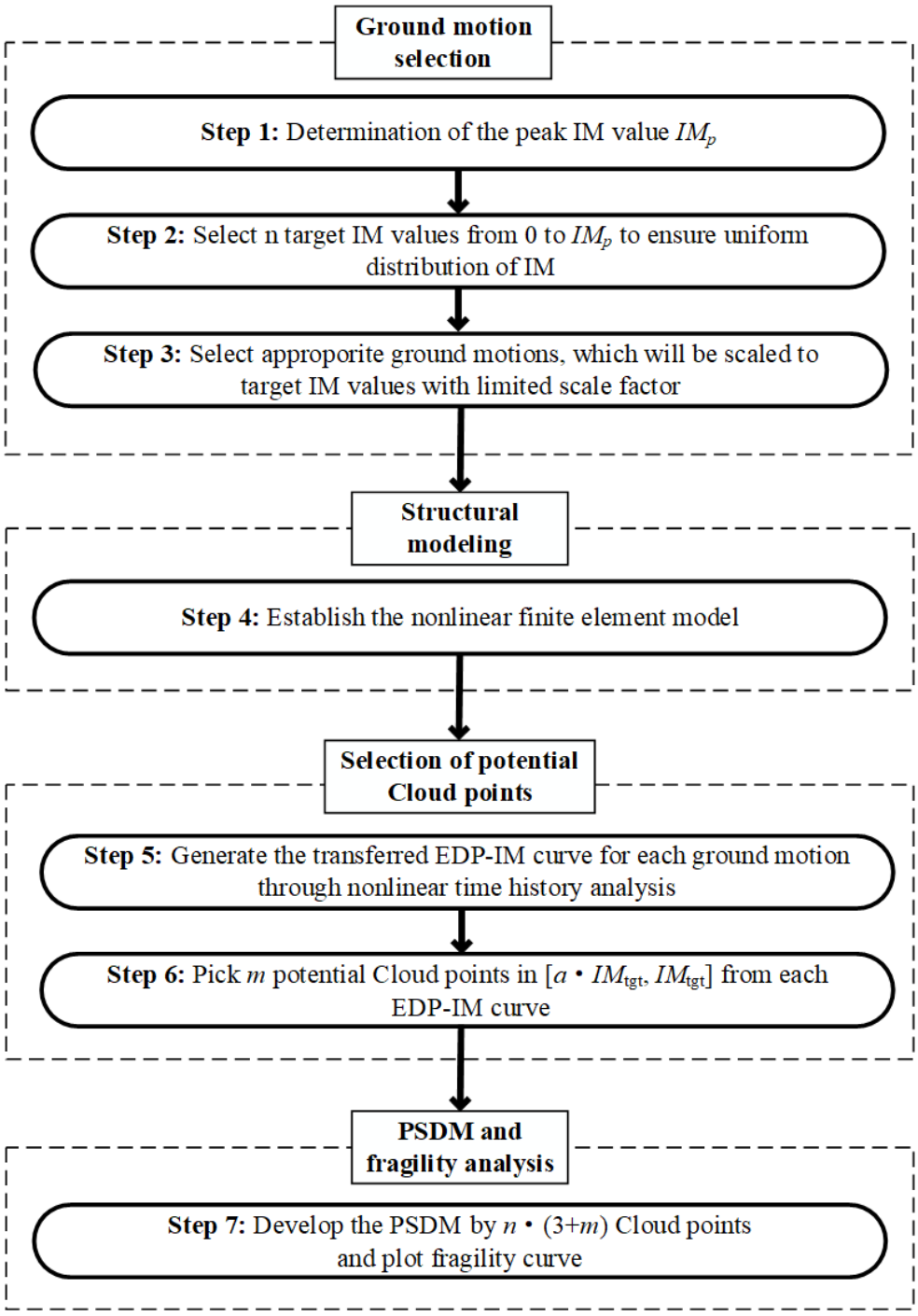

Figure 4

Flowchart of the “E-Cloud” method

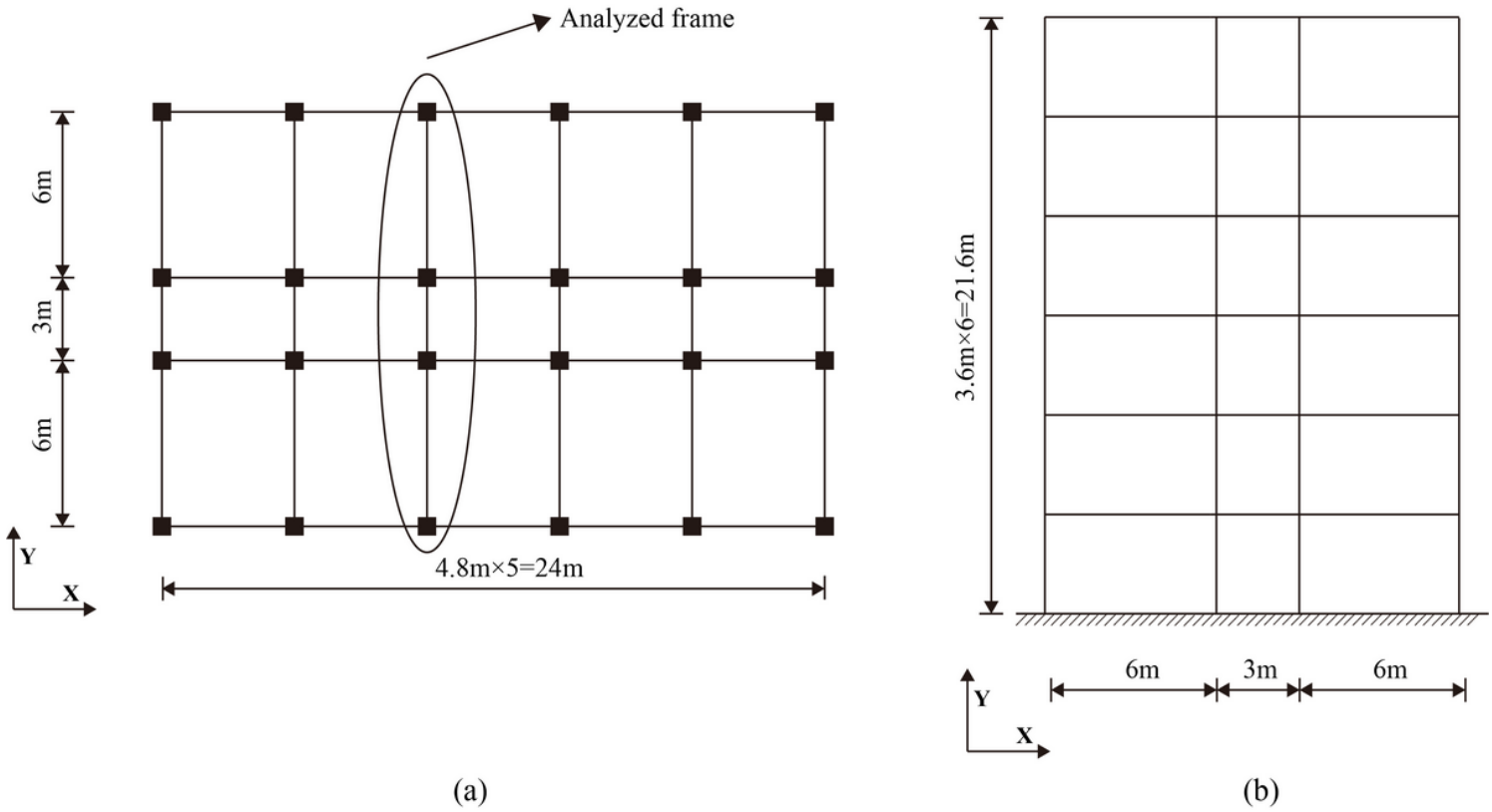

Figure 5

Schematic of the RC frame: (a) plan view, (b) elevation view

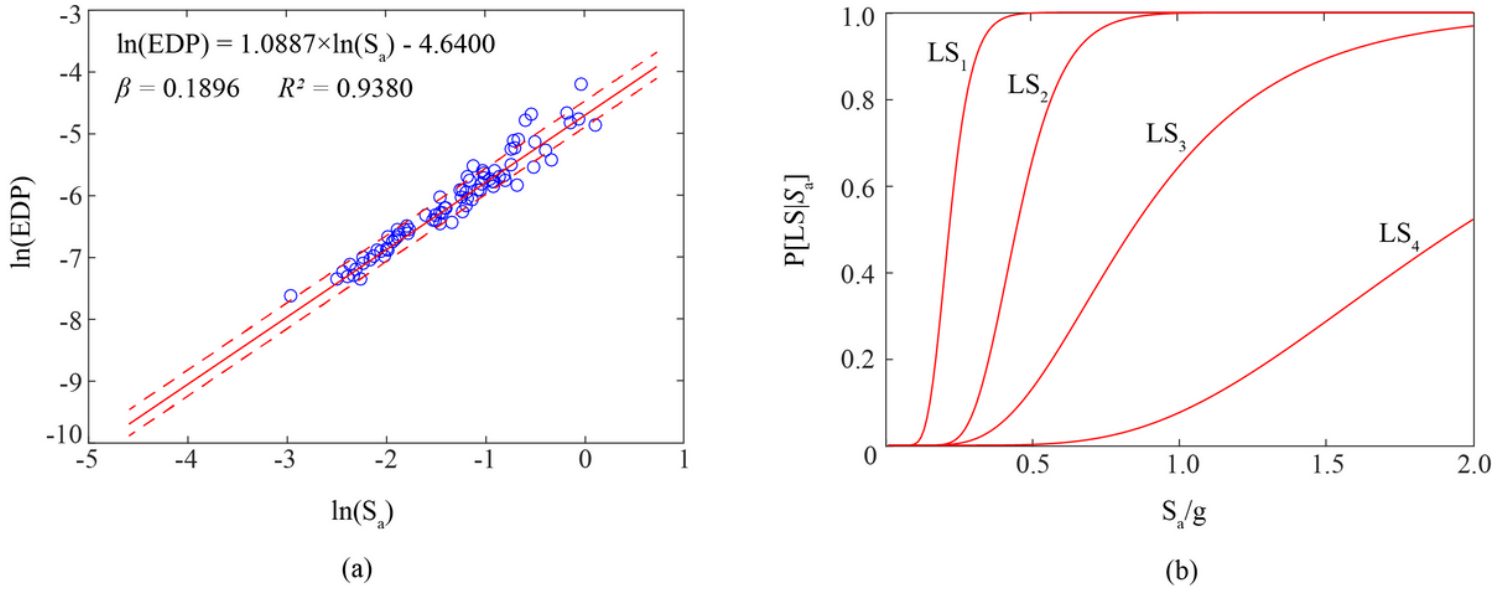

Figure 6

PSDM and fragility curves for Cloud analysis

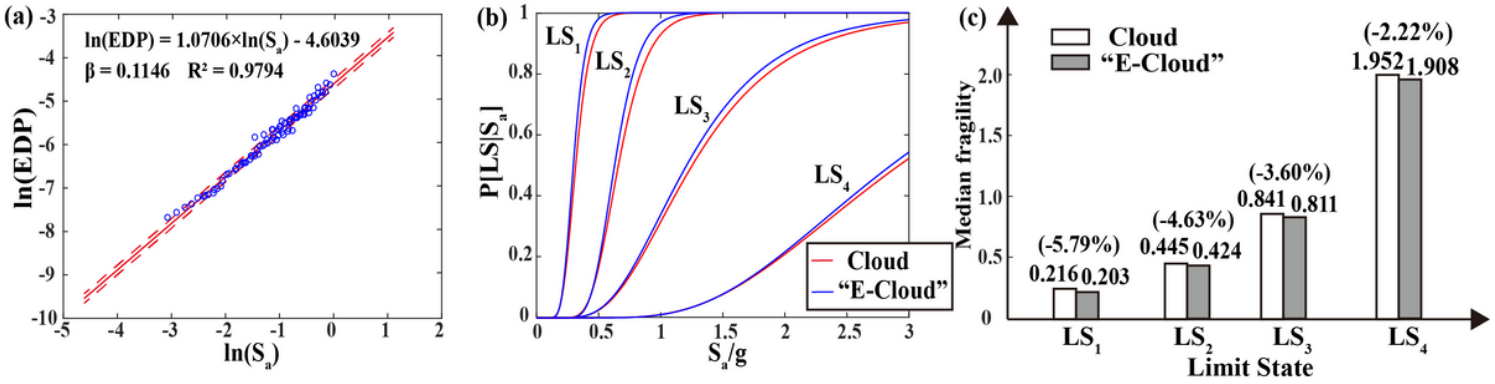

Figure 7

PSDM and fragility curves for "E-Cloud" method

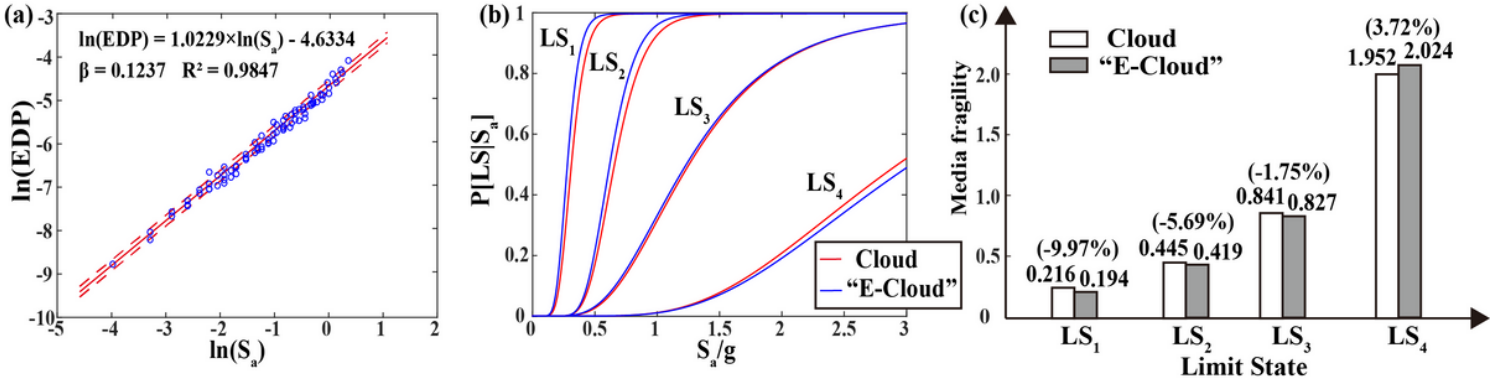

Figure 8

PSDM and fragility curves for "E-Cloud" method with a=0

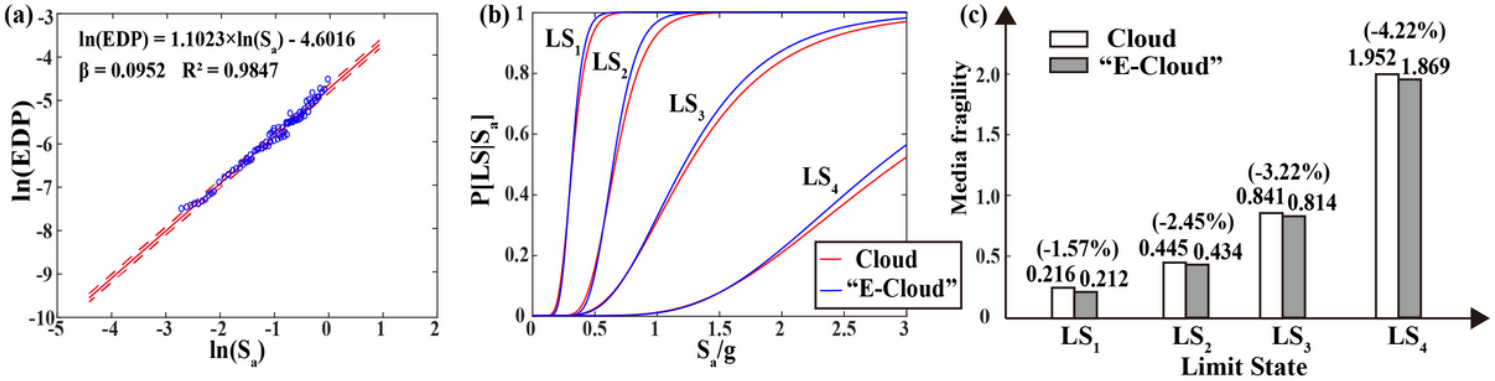

Figure 9

PSDM and fragility curves for "E-Cloud" method with a=0.5

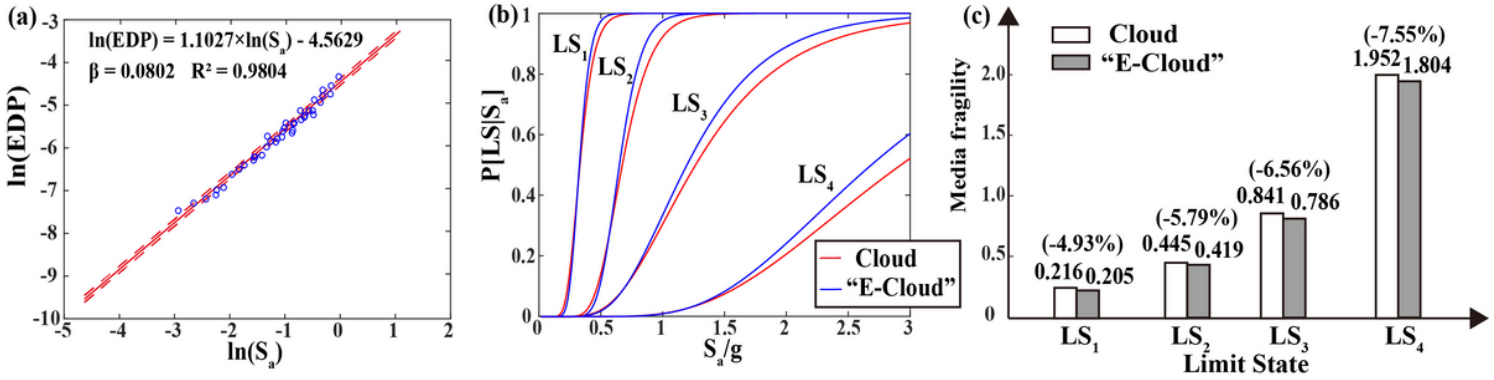

Figure 10

PSDM and fragility curves for "E-Cloud" method with m=5

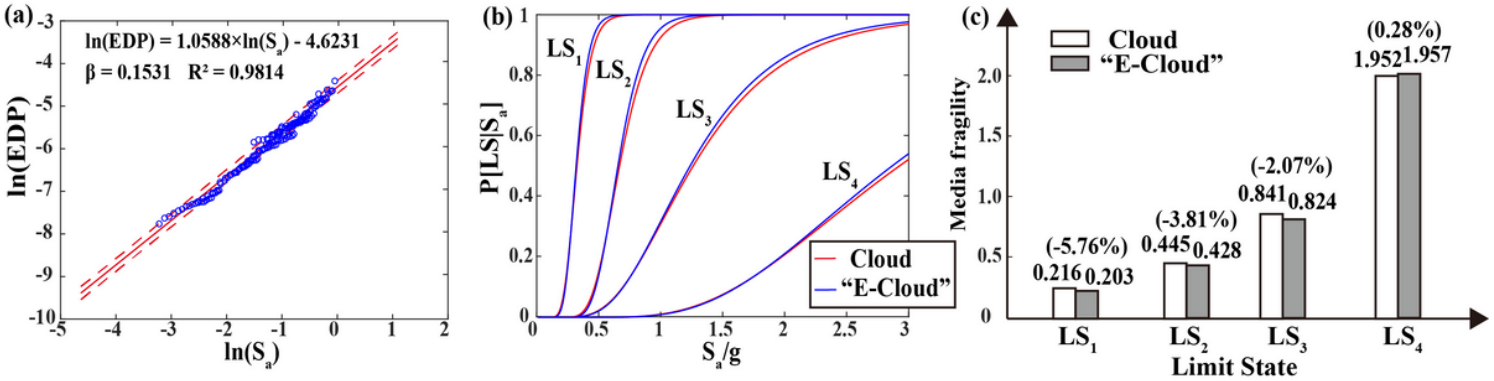

Figure 11

PSDM and fragility curves for "E-Cloud" method with m=20

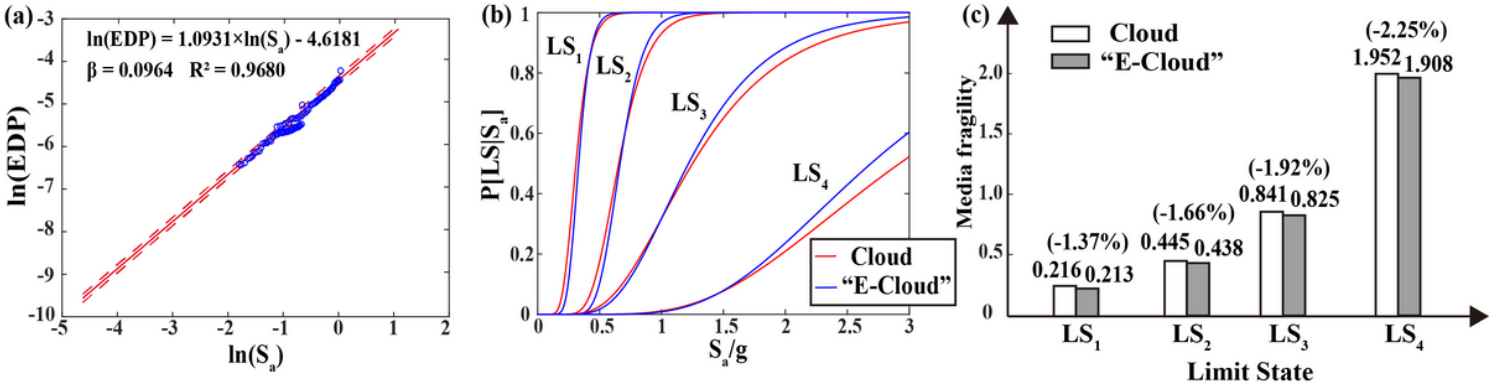

Figure 12

PSDM and fragility curves for "E-Cloud" method with n=2

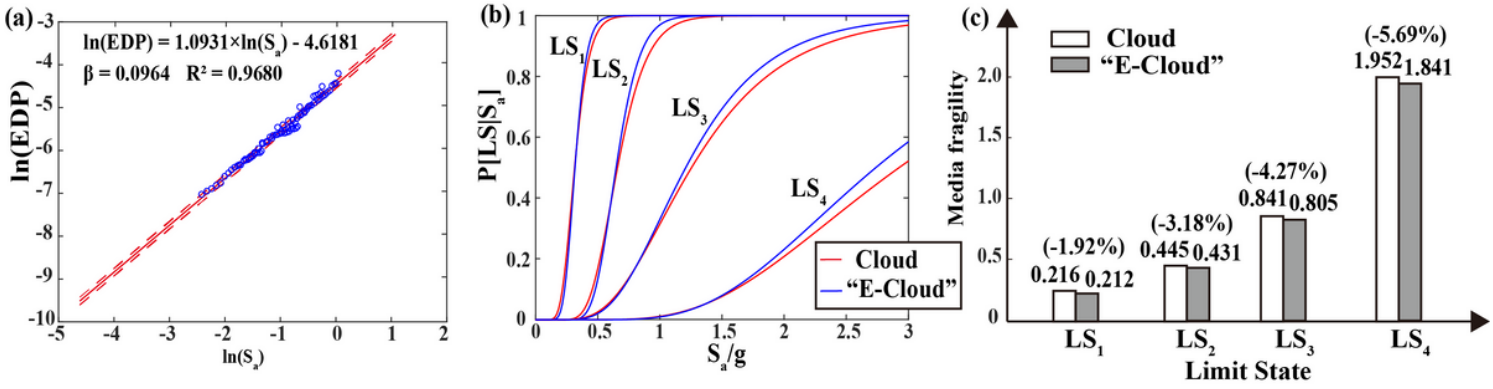

Figure 13

PSDM and fragility curves for “E-Cloud” method with n=4

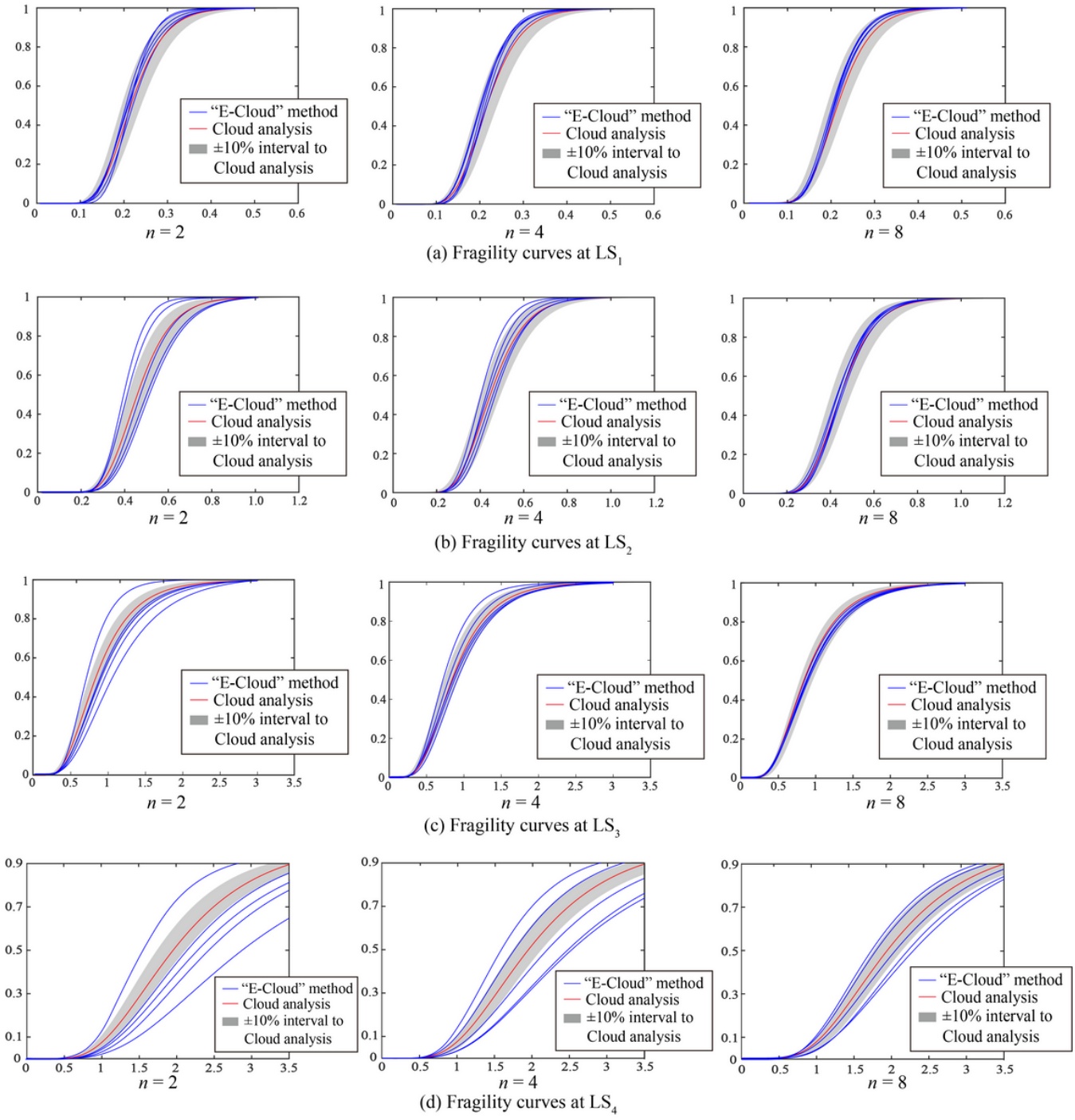

Figure 14

Fragility curves for group n=2, group n=4 and group n=8 at LS1(a), LS2(b), LS3(c) and LS4(d) by Cloud analysis and "E-Cloud" method